New Phytologist

Research

RNA-based analyses reveal fungal communities structured by a senescence gradient in the moss *Dicranum scoparium* and the presence of putative multi-trophic fungi

Ko-Hsuan Chen[1], Hui-Ling Liao[1,2], A. Elizabeth Arnold[3], Gregory Bonito[4] and François Lutzoni[1]

[1]Department of Biology, Duke University, Durham, NC 27708, USA; [2]Soil and Water Sciences Department, North Florida Research and Education Center, University of Florida, Quincy, FL 32351, USA; [3]School of Plant Sciences and Department of Ecology and Evolutionary Biology, University of Arizona, Tucson, AZ 85721, USA; [4]Department of Plant, Soil and Microbial Sciences, Michigan State University, East Lansing, MI 48824, USA

Author for correspondence:
Ko-Hsuan Chen
Tel: +1 850 875 7197
Email: *ko.hsuan.chen@duke.edu*

Received: *30 November 2017*
Accepted: *7 February 2018*

New Phytologist (2018) **218:** 1597–1611
doi: 10.1111/nph.15092

Key words: bryophyte, endophyte, fungal community, metatranscriptome, moss–fungus interaction, mycobiome, saprotroph, symbiotroph.

Summary

- Diverse plant-associated fungi are thought to have symbiotrophic and saprotrophic states because they can be isolated from both dead and living plant tissues. However, such tissues often are separated in time and space, and fungal activity at various stages of plant senescence is rarely assessed directly in fungal community studies.
- We used fungal ribosomal RNA metatranscriptomics to detect active fungal communities across a natural senescence gradient within wild-collected gametophytes of *Dicranum scoparium* (Bryophyta) to understand the distribution of active fungal communities in adjacent living, senescing and dead tissues.
- Ascomycota were active in all tissues across the senescence gradient. By contrast, Basidiomycota were prevalent and active in senescing and dead tissues. Several fungi were detected as active in living and dead tissues, suggesting their capacity for multi-trophy. Differences in community assembly detected by metatranscriptomics were echoed by amplicon sequencing of cDNA and compared to culture-based inferences and observation of fungal fruit bodies in the field.
- The combination of amplicon sequencing of cDNA and metatranscriptomics is promising for studying symbiotic systems with complex microbial diversity, allowing for the simultaneous detection of their presence and activity.

Introduction

Fungi that inhabit plant tissues comprise the plant mycobiome, and together they encompass diverse ecological modes ranging from saprotrophy to biotrophy (Peay *et al.*, 2016). Understanding the ecological and evolutionary dynamics of such fungi requires an understanding of both their distributions and activity in various plant tissues. Some fungi have been isolated independently from both dead and living plant tissues, suggesting that they may be able to exploit both living and nonliving plant material (U'Ren *et al.*, 2010; Osono & Hirose, 2011; Yuan & Chen, 2014; U'Ren & Arnold, 2016). *Lophodermium pinastri* is one such fungus: it lives as an endophyte inside symptomless pine needles, produces ascospores on fallen needles and can contribute directly to litter decomposition by degrading dead needles (Osono & Hirose, 2011). Nevertheless, the question remains: are such fungi latent saprotrophs, or can the same fungal strain live in a multi-trophic capacity – that is, be active as both a symbiotroph and a saprotroph? This question has proved difficult to answer, especially at a community level, because living and dead tissues often are separated in time and space and the biologically active fungi in tissues of each stage are rarely assessed simultaneously and in a systematic way. The most direct way to study fungal multi-trophism is to use plants with a continuous senescence gradient wherein different stages stay physically connected through time.

Mosses (phylum Bryophyta) often present a continuous senescence gradient, providing a unique opportunity to study fungal communities and their functions at distinct but proximate spatial and developmental scales. Mosses are widely distributed across diverse terrestrial biomes (Lindo & Gonzalez, 2010), where they play key roles in ecological processes including carbon and nutrient cycling (Brown & Bates, 1990; Turetsky *et al.*, 2012; Lenton *et al.*, 2016). Fungi associated with mosses include diverse parasitic, pathogenic, commensal, mutualistic and saprotrophic taxa (Redhead, 1981; Carleton & Read, 1991; Martínez-Abaigar *et al.*, 2005; Davey & Currah, 2006, 2007; Kauserud *et al.*, 2008; Davey *et al.*, 2010, 2013b, 2017; Stenroos *et al.*, 2010). Whereas ecto- and endo-mycorrhizal fungi can associate with mosses (Parke & Linderman, 1980; Davey & Currah, 2006; Zhang & Guo, 2007; Anderson *et al.*, 2014), typical mycorrhizal interactions between mosses and fungi are not common. By contrast,

mosses appear to commonly associate with fungal endophytes (U'Ren *et al.*, 2010, 2012; Yu *et al.*, 2014), but their trophic ecology awaits further investigation. Functions of moss-associated fungi are difficult to infer based on anatomical features alone, especially when obvious structures such as mycorrhizal-like structures or appressoria, indicative of infection or trophic modes, are lacking (but see Davey *et al.*, 2010).

Gametophytes of acrocarpous (i.e. erect-growing) mosses often have growth forms that comprise a senescence gradient consisting of three main layers: a photosynthetic layer at the top, a nonphotosynthetic layer in the middle and a decomposing layer at the base in contact with the soil (Fig. 1a). This growth form provides an opportunity to study fungal communities along a senescence gradient and to determine the active fungi in each layer. This system also circumvents several confounding issues with chronosequences in other settings, as the spatial scales are relatively small. With a focus on the transition zone between the top, healthy, photosynthetic layer and partly decomposed, bottom layer, such a system can potentially provide insight into functional and taxonomic turnover of microbes as plant tissues senesce.

Previous work on moss-associated fungi indicates that fungal communities often differ between living and dead tissue. For example, Davey *et al.* (2009, 2013a) compared ergosterol concentrations as an indicator of fungal biomass in the green (living) and brown (senescent) tissues of several moss species and noted that Basidiomycota fungi of the genera *Galerina* and *Mycena* were more prevalent in brown, dead tissues (Davey *et al.*, 2013b). A subsequent study (Davey *et al.*, 2017) based on amplicon sequencing data showed that distinct fungal communities occurred in photosynthetic and senescent tissues. There is a need to determine which fungi are active in each specific tissue layer, and across layers, to understand the symbiotrophic–saprotrophic continuum and the importance of multitrophism in plant–fungal symbioses.

Next generation sequencing (NGS), especially DNA amplicon sequencing of rRNA gene regions (e.g. the nuclear large subunit (nrLSU) and the internal transcribed spacer region (nrITS)), has greatly enhanced the understanding of fungal communities (Lindahl *et al.*, 2013; Tedersoo *et al.*, 2014; Davison *et al.*, 2015). However, communities that are metabolically active (more specifically, fungi with their rRNA being actively transcribed) can differ from those detectable via sequencing of DNA, which can include fungi that are in a dormant state or dead (Rajala *et al.*, 2011; Baldrian *et al.*, 2012; Barnard *et al.*, 2013; Liao *et al.*, 2014). Similarly, read counts obtained through amplicon sequencing may not reflect actual abundances of taxa (Amend *et al.*, 2010; Nguyen *et al.*, 2015). Shotgun sequencing of metagenomic DNA and metatranscriptomic RNA can diminish biases associated with amplicon sequencing (Lindahl *et al.*, 2013; Tedersoo *et al.*, 2015), as these methods involve fewer PCR amplification cycles (e.g. the Illumina TruSeq stranded mRNA preparation kit includes 15 cycles of PCR amplifications, with primers annealed to the Illumina adaptors) and are less subject to primer bias toward certain taxa (Choma *et al.*, 2016). When applying RNA-based detection methods, rRNA transcripts often are used as proxies for active living proportions, and effective abundances, of fungal communities (Baldrian *et al.*, 2012; Liao *et al.*, 2014; Hesse *et al.*, 2015; Mueller *et al.*, 2015). Some biases are inevitable (e.g. variation of rRNA copy numbers among fungal taxa), but this approach can be applied to plant mycobiomes as a first step to discover fungi that are both present and active in different tissue types. In doing so, fundamental questions regarding the functional and taxonomic continuity of fungal communities under different ecological circumstances (e.g. tissue senescence) can be addressed simultaneously.

Here we combined metatranscriptomic analyses of fungal rRNA, amplicon sequencing of cDNA, culturing and fruit-body collections in naturally occurring gametophytes of the moss *Dicranum scoparium* to better understand the distribution and activity (in the sense of their rRNA genes being actively transcribed) of fungi at small spatial scales across a gradual senescence gradient. We addressed the following hypotheses: active fungal communities change along the senescence gradient; and some fungi are active in all tissues at different stages of senescence, potentially corresponding to trophic shifts between symbiotrophy and saprotrophy (i.e. they are multitrophic fungi). To test these hypotheses, we collected *D. scoparium* gametophytes from their natural habitat and sampled plant tissues from replicated senescence gradients (Fig. 1a,b). Analyses ordinarily used for detecting differentially expressed genes (DEGs) and community assemblies were implemented in the context of an integrated workflow (Fig. 1c) by which results from different approaches can be readily compared (metatranscriptomic data from shotgun NGS reads, amplicon sequencing of cDNA using PCR-based NGS reads, and both endophyte cultures and fruit-bodies evaluated using PCR-based Sanger sequencing). Previous studies have used rRNA transcripts in metatranscriptomic data for community analyses of fungi (Liao *et al.*, 2014), protists (Geisen *et al.*, 2015), and Archaea and Bacteria (Lesniewski *et al.*, 2012). Here we compared this approach to other standard methods (amplicon sequencing of cDNA and Sanger sequencing, both of endophytes isolated in culture and fruit-bodies).

Materials and Methods

Moss mats (30 × 30 cm) with attached soil were collected in January 2014 at three microsites (10 m apart from the central microsite) along a 20 m transect consisting of a uniform stand of *Dicranum scoparium* gametophytes in Duke Forest, near Durham, NC, USA (36.010830°N, 78.967864°W; Fig. 1b). Duke Forest is a mixed hardwood–coniferous forest where mosses are abundant. Together the collections from three microsites represented the standard three biological replicates for transcriptomic analysis (Love *et al.*, 2014), and they are numbered 1–3 in our workflow scheme (Fig. 1a–c).

We collected nine samples from the moss collections (Fig. 1). Three samples were from the top layer of the gametophytes (t1–t3); these were green and apparently healthy. Three were from the middle layer of the gametophytes (m1–m3), representing a transition zone from green to senescent tissue. The remaining three were from the bottom layer of the gametophytes (b1–b3),

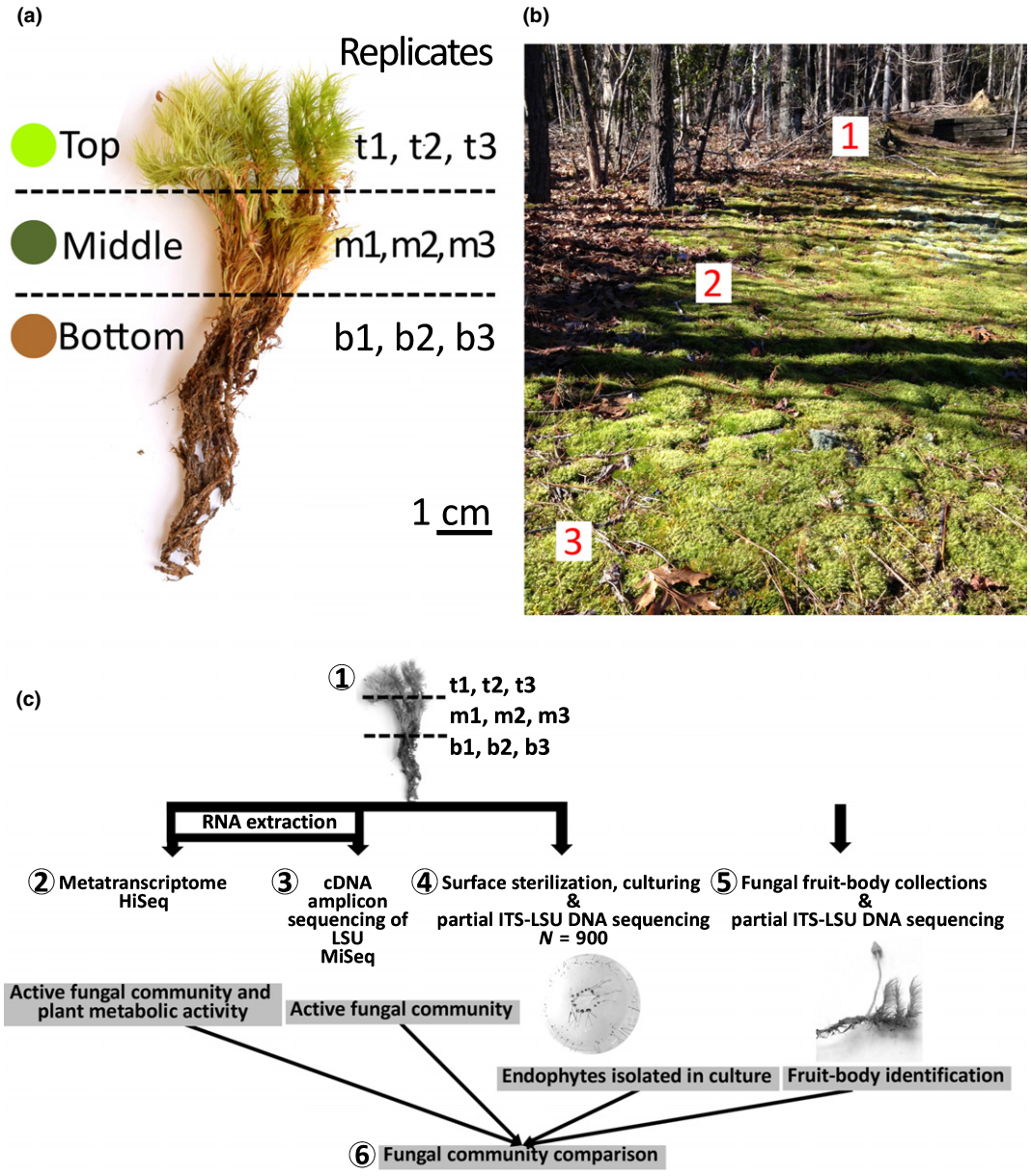

Fig. 1 (a) Senescence gradient of *Dicranum scoparium*. The color key and names of the replicates for the top (t1–t3), middle (m1–m3) and bottom (b1–b3) layers are applied throughout this study. (b) Sampling site in Duke Forest, North Carolina, showing the collecting scheme (three microsites with two intervals of 10 m). (c) Schematic overview of sampling and methods. Moss sampling (step 1), systematic data acquisition for metatranscriptome (step 2), cDNA amplicon sequencing (step 3), isolation of endophytes in culture (step 4), fruit-body (sporocarp) collections (step 5) and fungal community comparison (step 6).

where the tissue was fully senesced and brown. Each sample contained *c.* 20 moss stem sections.

RNA extraction and culture-free methods

The overall workflow for tissue processing and molecular analysis is shown in Fig. 1(c). For the culture-free approaches, gametophytes at the edge of each moss mat were discarded and those in the center were submerged in liquid nitrogen immediately after collection. To avoid interference with RNA activity, surface sterilization was not performed. Gametophytes then were cut and sorted into top, middle and bottom layers, and stored at −80°C. Samples were ground with a ceramic mortar and pestle in liquid nitrogen immediately before RNA extraction with RNAqueous Total RNA Isolation Kit/Plant RNA Isolation Aid (Thermo Fisher Scientific, Waltham, MA, USA). Procedures for RNA extraction were based on the manufacturer's protocol except for the addition of a DNase incubation step (D. Armaleo, personal communication). Approximately 100–250 mg (wet weight) of gametophyte fragments was used per RNA extraction.

RNAseq libraries for metatranscriptomes were prepared using the Illumina TruSeq Stranded mRNA library Prep kit following the manufacturer's protocol, and were sequenced with Illumina

HiSeq (Fig. 1c, step 2; Supporting Information Methods S1). Amplicon sequencing was performed using the same RNA extractions, focusing only on microsites 2 and 3 (Fig. 1c, step 3). The RNA was reverse transcribed to a cDNA library using the SuperScript II Reverse Transcriptase kit (Sigma) with the LR3 primer (Vilgalys & Hester, 1990) (Methods S2). Amplicon libraries were then prepared for the nrLSU rDNA region with primers LR0R-LR3 (targeting the D1/D2 region; Vilgalys & Hester, 1990) and were sequenced with Illumina MiSeq. The D1/D2 regions were targeted because they are variable regions that have been used extensively for DNA barcoding of fungi (Seifert, 2009; Schoch *et al.*, 2012). Library preparation for amplicon sequencing utilized a frame-shift tagging system in the primer sequence (Lundberg *et al.*, 2013) to generate high-diversity libraries necessary for MiSeq sequencing, thus eliminating the need for Phi X spiking before sequencing. Amplification consisted of three PCR amplification steps, which were optimized to reduce primer-dimer and nonspecific amplification (Methods S2). The first 'enrichment' amplification round was done to enrich for the region being amplified and consisted of 10 PCR cycles with the general LR0R and LR3 primers (Table S1) (Vilgalys & Hester, 1990). The second 'tagging' round of amplification was carried out to tag amplicons with Illumina bridge-PCR adapters, and consisted of 10 PCR cycles with modified LR0R and LR3 primers (Methods S2; Table S1). A third round of amplification was carried out to PCR-ligate sample-specific Illumina indices and consisted of 10 PCR cycles. Sample-specific indices consisted of 10 bp sequences derived from Golay primers and consisting of nonbiased ratios of nucleotides (Methods S2; Table S2). Illumina sequencing primers submitted with the MiSeq libraries are provided in Table S3.

Bioinformatics workflow for RNAseq and cDNA-amplicon sequencing

Raw reads of RNAseq data were processed to trim adaptors and were quality filtered using Trimmomatic (Bolger *et al.*, 2014) (Methods S3; Table S4). Reads obtained from amplicon sequencing of cDNA were processed by quality filtering with Usearch (Edgar, 2013). All reads were truncated to 150 bp with the maximum error rate allowance of 0.25 (Methods S4; Fig. S1). For scripts used for data processing, see Methods S5.

Reference library preparation for metatranscriptomics

For metatranscriptomic analyses of *D. scoparium*, two reference datasets were used: *Physcomitrella patens* genome v.3.0 (Zimmer *et al.*, 2013) and *Dicranum scoparium* EST (Li *et al.*, 2014). For the fungal rRNA reference library, primary libraries were created from public resources and project-related data for LR0R and LR3 (Figs S2a, S3a; Methods S6). After primer trimming, only the first 250 bp was kept for reference sequences to ensure all reads mapped were restricted to the same region. This allowed overlap of rRNA contigs extracted from metatranscriptomics with those produced via amplicon sequencing and Sanger sequencing. Secondary libraries were created using the reads mapped by Bowtie2 (Langmead *et al.*, 2009) to the primary library from the *D. scoparium* metatranscriptome. These reads were either assembled with Velvet (Zerbino & Birney, 2008) or merged as pairs via Usearch (Edgar, 2013), and therefore were referred to as metatranscriptome assembled (MA) and metatranscriptome pair-merged (MP) databases, respectively.

After the assembly or merging process, sequences were clustered into operational taxonomic units (OTUs) at 97% sequence similarity with Usearch (Edgar, 2013) and aligned using Mafft (Katoh & Standley, 2013) (Methods S5, S6). The 97% similarity threshold was chosen because it is suggested in the Uparse pipeline (Edgar, 2013), and has been used in analyses of the D1/D2 region for fungi in several studies (Bonito *et al.*, 2014; Porras-Alfaro *et al.*, 2014; Mueller *et al.*, 2016). To test whether different cutoffs impacted our results, we assessed the impact of clustering the LR3-MP dataset at 95% compared to 97% sequence similarity. D1 and D2 regions were targeted by primers LR0R and LR3 separately to avoid reads being mapped to different regions and consequently affecting secondary library constructions and OTU circumscriptions.

Analyses and visualization of fungal rRNA transcription levels across a senescence gradient

We detected DEGs with the R package DEseq2 (Love *et al.*, 2014) to identify biologically active fungi in each layer for metatranscriptomic datasets (LR0R-MP, LR0R-MA, LR3-MP, LR3-MA). Wald tests were performed to detect taxa with significant differential abundance (adjusted P-value < 0.05). Taxa with adjusted P-value > 0.05 and $\log_2$ fold change < 1 were interpreted as not differentially abundant across layers. Values for heat maps were calculated by read counts transformed by the Variance Stabilizing Transformation (VST) function in DEseq2. The read counts for cDNA amplicon sequencing and culture-based datasets (LR0R-amp, LR3-amp and culture) were also transformed using the VST technique (Love *et al.*, 2014) in Qiime (Caporaso *et al.*, 2010). Taxonomy was assigned through MegaBlast against the NCBI database (excluding uncultured and environmental sequences) and the top 50 hits were recorded for Megan v.5.10.6 (Huson *et al.*, 2007) to report the lowest common ancestor (LCA). We used a minimum score = 150, top percentage = 20 and LCA per cent = 50 to report LCAs, and LCAs were constrained to the genus level (without species or strain information). A second taxonomic assignment was generated with the RDP classifier (bootstrap percentage = 70%) (Liu *et al.*, 2012; Porras-Alfaro *et al.*, 2014). Qiime (Caporaso *et al.*, 2010) was used to summarize taxonomic composition, calculate abundance-based beta diversity (Bray–Curtis dissimilarity), perform non-metric multidimensional scaling (NMDS) analysis and normalize matrices (see scripts in Methods S5) for all datasets. Rarefaction curves were generated to examine the evenness of sequencing depth, and sampling depths were set as the lowest number of reads in Qiime for the given datasets. To assess whether community differences along the senescence gradient

could be attributed to taxa replacement or loss, the turnover and nestedness components of the presence/absence-based Sørenson beta-diversity index were calculated with the R package BETAPART (Baselga, 2010) for LR0R-MP and LR0R-amplicon comparisons (see scripts in Methods S5).

Statistical tests

To test the relationship of layer type to beta-diversity and community composition, we performed a nonparametric version of permutational multivariate analysis of variance (Anderson, 2001) using the ADONIS function in the VEGAN package (Oksanen *et al.*, 2015). Chi-square tests were performed to investigate whether the ratio of reads mapped to fungal rRNA datasets were independent from the sampling layers. For the comparison of taxa across layers, raw read counts were normalized following the pseudo-count method in EDGER (Robinson *et al.*, 2009). In the two-way ANOVAs, we grouped fungi belonging to their highest taxonomic rank (phyla or subphyla levels) into a single category (phylumFactor). Two-way ANOVA was conducted to test the null hypothesis that the mean of read counts was the same for all phylumFactors ($\mu_{phylumFactor1} = \mu_{phylumFactor2} \ldots = \mu_{phylumFactor\_n}$), and were the same across the three layers (top, middle, bottom, $\mu_t = \mu_m = \mu_b$). When interactions between the two factors (phylumFactor and layer) were detected, we were unable to interpret these two factors separately. Therefore, one-way ANOVAs were performed subsequently on individual phyla and subphyla to test the null hypothesis that mean read counts are the same for a particular phylum or subphylum across three layers (top, middle, bottom, $\mu_{t,phylum/subphylum} = \mu_{m,phylum/subphylum} = \mu_{b,phylum/subphylum}$). All datasets were subjected to tests of normality (Shapiro–Wilk) and homogeneity of variance (Fligner–Killeen). The false discovery rate (FDR) correction was applied when multiple comparisons were made within a dataset. Statistical analyses were not performed on the cDNA amplicon sequencing datasets (LR0R-amp and LR3-amp) because these datasets contained only two replicates.

Isolation of endophytic fungi in pure culture

Within 6 h of field collection, material from each moss mat was dissected into the top, middle and bottom layers (Fig. 1c, step 1). Each mat was surface-sterilized following U'Ren *et al.* (2012) and cut into 100 tissue fragments per layer (*c.* 2–3 mm^2 each). Fragments were plated on 2% malt extract agar (MEA) for a total of 900 fragments (Fig. 1c, step 4). Fungal growth was monitored for 1 yr. Each emergent strain was transferred to a new plate and a living voucher was preserved in sterile water at room temperature (U'Ren *et al.*, 2010). Fungal hyphae also were observed inside photosynthetic tissues under a dissecting microscope, after the plant tissues were made more transparent by soaking in a 3% KOH solution overnight and staining with Trypan blue.

Field collections of fruit-bodies

The field site was surveyed for visible fungal fruit-bodies associated with *D. scoparium* 12 times over a 1-yr period (November 2014–October 2015), especially following rainy periods (Fig. 1c, step 5). Fruit-bodies were collected and air-dried in the lab. Before air-drying, spore prints were collected and attempts were made to obtain fungal cultures using MEA and modified Melin–Norkrans medium (Marx, 1969). Gametophytes also were kept in sealed beakers (moist chambers) in the lab to foster development of fungal fruit-bodies. The nrITS–partial nrLSU region was sequenced for fruit-bodies and isolates derived from them.

Genotyping fungal isolates and fruit-bodies

DNA was extracted from fungal isolates (above) and sporocarps (fruit-bodies) using Tris-EDTA buffer (Oono *et al.*, 2014). The primer set ITS1F (Gardes & Bruns, 1993) and LR3 (Vilgalys & Hester, 1990) was used to PCR-amplify all isolates following U'Ren *et al.* (2012). A two-step process was used to determine which isolates should be sequenced. First, each fungal isolate was assigned to a morphogroup based on observable phenotypic traits when grown on MEA. Second, restriction fragment length polymorphism (RFLP) patterns using MSPI (CCGG 5′-CG) and Eco0109 (RGGNCCY 5′-GNC; New England BioLabs Inc., Ipswich, MA, USA) of PCR products were visualized through 2% agarose gel electrophoresis (Oono *et al.*, 2014). These restriction enzymes were chosen based on an alignment of the first 36 isolates sequenced, and were confirmed to yield different RFLP patterns for each OTU delimited based upon 95% similarity (U'Ren *et al.*, 2009, 2010, 2012, 2014) as implemented in SEQUENCHER v.5.3 (Gene Codes Corp., Ann Arbor, MI, USA). Morphogroups and RFLP patterns were compared and at least two strains from each RFLP group, and strains showing conflicts between the two grouping methods, were sequenced. Before sequencing, PCR products were cleaned with both Exonuclease (Affymetrix, Santa Clara, CA, USA) and Antarctic Phosphatase (New England Biolabs). Sequencing was performed using BigDye v.1.1 system for dual directions (ITS1F forward and LR3 for reverse) and analyzed with an ABI 3730xl at the Duke Center for Genomic and Computational Biology. Sequences were assembled and their quality was inspected using SEQUENCHER v.5.3. All newly generated sequences were submitted to NCBI (accession numbers MF942878–MF943126).

Comparison of OTUs detected through metatranscriptomics, amplicon sequencing, culturing and fruit-body collections

The LR0R-MP dataset and all sequences of endophytes isolated in culture and fruit-bodies were trimmed to 150 bp after the LR0R primer and pooled with LR0R amplicon sequences. These sequences were barcoded to correspond to their detection methods (metatranscriptome, amplicon sequencing or isolated endophytes/fruit-body collections). Singletons in the amplicon sequencing data were removed before pooling. USEARCH was used to cluster pooled sequences into OTUs following a 97% and 95% sequence similarity criterion (Edgar, 2013) (Methods S5). The original data were mapped to the representative OTU with USEARCH (Edgar, 2013) following a 97% or 95% sequence

similarity according to the cutoffs set for OTU delimitation. This step generated an OTU table, and shows the OTUs detected by different methods (i.e. metatranscriptome vs amplicon sequencing vs culture-based and fruit-body collection). This comparison was conducted only on the LR0R dataset because far fewer reads were retained from LR3 amplicon sequencing (Fig. S1).

Results

Metatranscriptomic assessment of plant and fungal activities across a senescence gradient

Our sampling strategy captured the declining activity of *D. scoparium* along the senescence gradient from the photosynthetic layer at the top to the decomposing layer at the bottom. The ratios of the RNA reads belonging to *D. scoparium* (of the remaining reads after quality control) decreased along this gradient (Fig. S4; read quality is shown in Table S4). Regardless of the fungal rRNA dataset used (LR0R (primary, MA, MP) or LR3 (primary, MA, MP)), the ratios of mapped fungal rRNA reads differed among layers (Chi-square test: $P < 1e\text{-}10$, Table S5). The overall trend was of increasing fungal rRNA transcripts toward the bottom layers (Figs S2b, S3b).

Community assemblies of active fungi across the senescence gradient

Beta-diversity (Bray–Curtis dissimilarity) of the LR0R-MA and LR0R-MP datasets showed that active fungal communities differed significantly along the senescence gradient (Fig. 2a,d) (ADONIS for LR0R-MP: $P = 0.021$; LR0R-MA: $P = 0.019$, Table S6). The percentage of OTUs assigned to the genus and order level ranged from 32% (LR0R_amp) to 58% (LR3_MA), and 72% (LR0R_amp) to 96% (LR3_MA), respectively. Beta-diversity based on LR0R and LR3 amplicon sequencing revealed the same pattern (Fig. 2c,f). The OTU tables of different datasets are given in Tables S7–S10 (metatranscriptomic) and Tables S11 and S12 (cDNA amplicon sequencing). The presence/absence-based Sørenson diversity index suggested that different fungal communities detected across layers were explained more by species replacement (turnover) than loss (nestedness) except for the LR0R-MP dataset at microsite 2 (Table S13).

Differential rRNA transcription level of the living proportions of fungal OTUs based on metatranscriptomic rRNA

Seventeen OTUs were more abundant and active in the bottom layer vs the top layer. By contrast, only four OTUs were more abundant and active in the top layer vs the bottom layer (Fig. 3a–d; Table S14). OTUs representing several taxa were detected in multiple datasets as being not differentially active across the three layers (e.g. a Herpotrichiellaceae species, *Hyalocypha*, as well as *Sistotrema*, *Epibryon*, *Mortierella*, *Cladosporium* and fungi of the order Helotiales; Fig. 3e–h). Although the four datasets revealed slightly different results, most of the results were complementary and did not contradict one another notably (Fig. 3; Table S14). However, there were OTUs with taxonomic affiliations that were detected as being differentially and nondifferentially active in different datasets (Fig. 3). The proportions of the OTUs that are

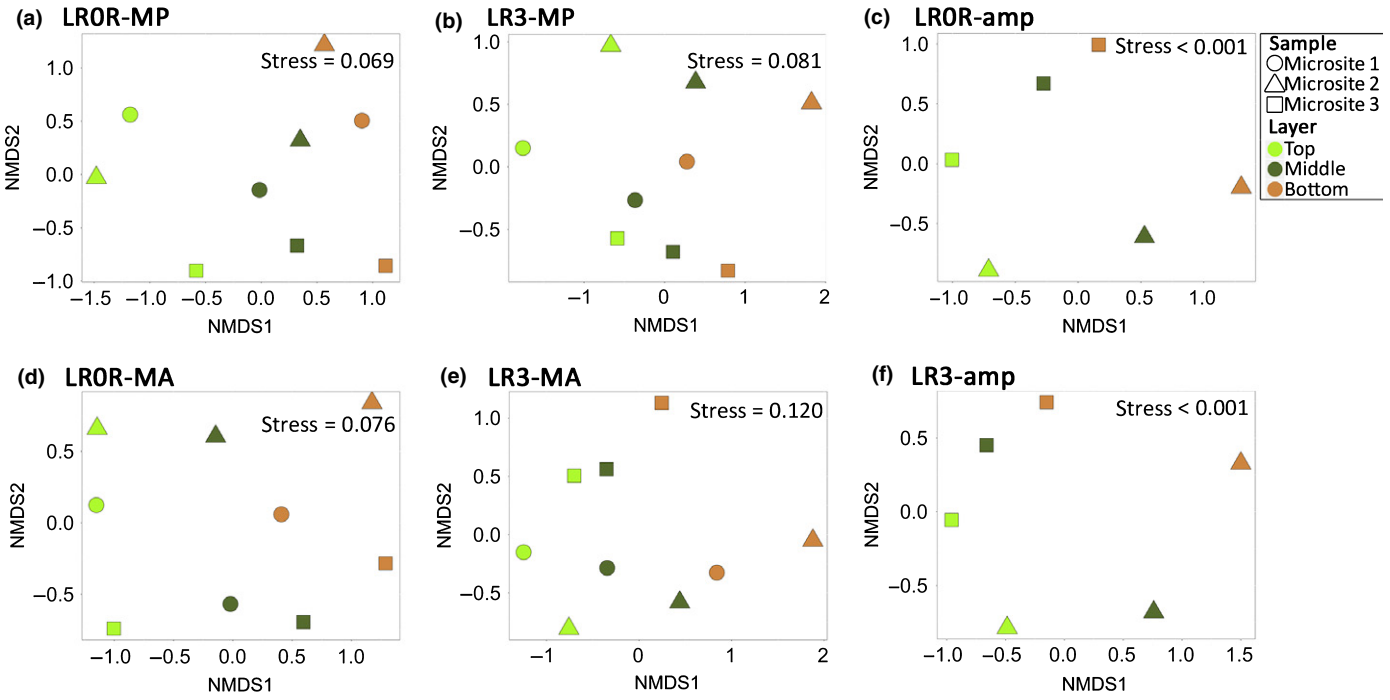

Fig. 2 Nonmetric multidimensional scaling (NMDS) plots based on Bray–Curtis dissimilarity matrix for metatranscriptome rRNA (a, b, d, e) and amplicon-sequencing of cDNA (c, f). (a, d) NMDS plots of LR0R-MP and LR0R-MA. (b, e) NMDS plots of LR3-MP and LR3-MA. (c, f) NMDS plot of amplicons sequenced with LR0R and LR3. MA, metatranscriptome assembled; MP, metatranscriptome pair-merged; amp, amplicon sequencing.

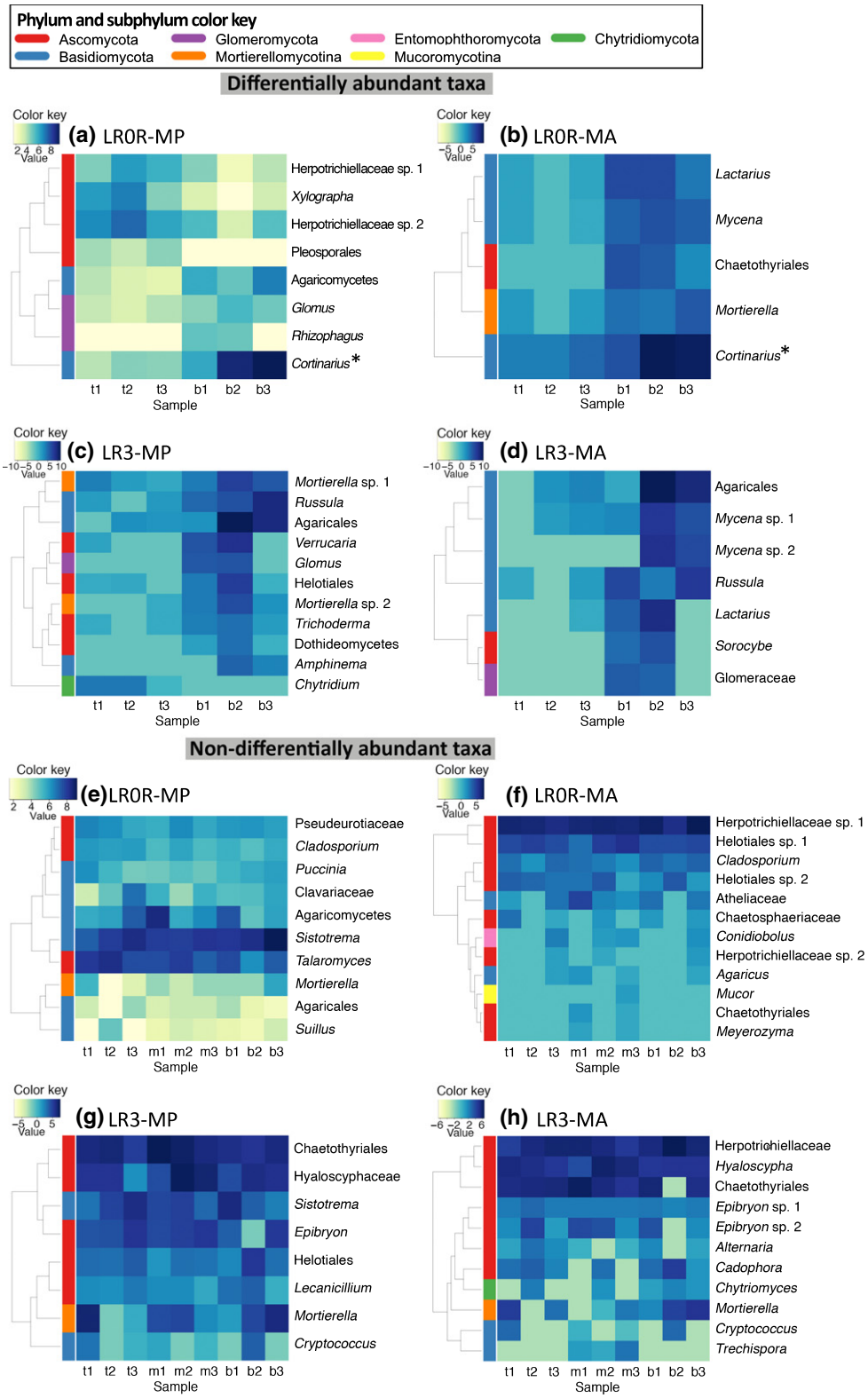

Fig. 3 (a–d) Operational taxonomic units (OTUs) detected as differentially abundant (OTU selecting criteria: Wald test, $P < 0.05$) in the top vs bottom layers of *Dicranum scoparium* with LR0R and LR3 (metatranscriptome assembled (MA) and metatranscriptome pair-merged (MP) databases). (e–h) OTUs detected as not differentially abundant across layers of *D. scoparium* (OTU selecting criteria: Wald test, $P > 0.05$, $\log_2$ fold change < 1) with LR0R and LR3 (MA and MP databases). Row labels on the right indicate the last common ancestor (lowest common ancestor (LCA); i.e. genus to class). When the same taxon name appears twice in one panel, this indicates the detection of two distinct OTUs. The colored blocks at the tip of the dendrogram indicate the phylum or subphylum of each OTU (see legend). The color key of the heatmaps corresponds to the transformed read counts mapped to specific OTUs. **Cortinarius* = *Galerina*, see Supporting Information Methods S7. t1–t3, top layers; m1–m3, middle layers; b1–b3, bottom layers.

capable of inhabiting more than one layer (selecting criteria: Wald test, $P > 0.05$, $\log_2$ fold change < 1) ranged from 9% (LR3_MP) to 26% (LR0R_MP).

Endophytes isolated in culture, and fruit-bodies

A total of 398 fungal isolates were obtained from 900 surface-sterilized gametophyte pieces of *Dicranum scoparium*. These isolates represented 61 OTUs based on a 95% sequence similarity criterion (U'Ren *et al.*, 2009) (Tables S15, S16). Replicates 1 and 2 had a higher isolation frequency in the top layer compared to the middle and bottom layers, but replicate 3 decreased in isolation frequency from the bottom to the top layer (Fig. S5). Fungal hyphae were abundant in photosynthetic tissues of *D. scoparium* (Fig. S6).

Thirty-one fruit-bodies were collected from *D. scoparium* in the field or after gametophytes were incubated in the lab (Table S17), and most (27 of 31) were Basidiomycota. Basidiomata of *Rickenella*, *Galerina* and *Mycena* were repeatedly found attached to *D. scoparium* gametophytes (Fig. S7). Basidiomata of ectomycorrhizal fungi were also detected at the site (e.g. *Russula*, *Suillus* and *Chroogomphus*) but were not physically attached to gametophytes. Apothecia of unidentified ascomycetous fungi were found growing directly on gametophytes at collection or developed after incubation. *Elaphocordyceps*, known to parasitize the ectomycorrhizal fungus *Elaphomyces*, was collected once. No perithecium was found on *D. scoparium*, despite careful evaluation with a dissecting microscope.

Taxonomic composition of fungal communities

Based on metatranscriptomic and cDNA-amplicon sequencing data, Ascomycota appeared to be more abundant in the top (green, living) layer and Basidiomycota more abundant in the bottom (senescent) layer of *D. scoparium* gametophytes (Fig. 4a–f). Results of two-way ANOVA detected interactions between layer and phylumFactor (layer : phylumFactor $P < 0.05$, Table S18) when all taxa at these levels were considered simultaneously. Therefore, it is invalid at this taxonomic level to interpret the differences of all taxa globally among layers (layer $P > 0.99$) (Table S18). Some of the results from the one-way ANOVA performed on each individual phylum or subphylum using metatranscriptomic data were statistically significant. However, after FDR correction, these *P*-values were slightly above 0.05 (Table S19). This trend was also observed for Ascomycota endophytes isolated in culture from two of the three replicates (Fig. 4g).

Entomophthoromycota were detected only with LR0R primers for both the metatranscriptomic and the amplicon sequencing experiments, whereas Chytridiomycota were detected only by LR3 with metatranscriptomics, but with both LR0R and LR3 by amplicon sequencing (Tables S7, S9, S11, S12). Two phyla (Entomophthoromycota and Chytridiomycota) and two subphyla (Glomeromycotina and Mucoromycotina) were detected by metatranscriptomic and/or amplicon sequencing but not by our culture-dependent method (Tables S7–S12).

Agaricomycetes, Eurotiomycetes and Leotiomycetes were abundant, but the Agaricomycetes proportionally increased while the latter two classes decreased toward the bottom in most metatranscriptomic and amplicon sequencing datasets (Fig. 4h–m). Sordariomycetes often dominated the endophytes obtained in culture from surface-sterilized samples (Fig. 4n) but they were detected rarely with LR3-metatranscriptomics and rRNA amplicon sequencing. Eurotiomycetes were abundant in all datasets (i.e. metatranscriptome, amplicon sequencing and endophytes

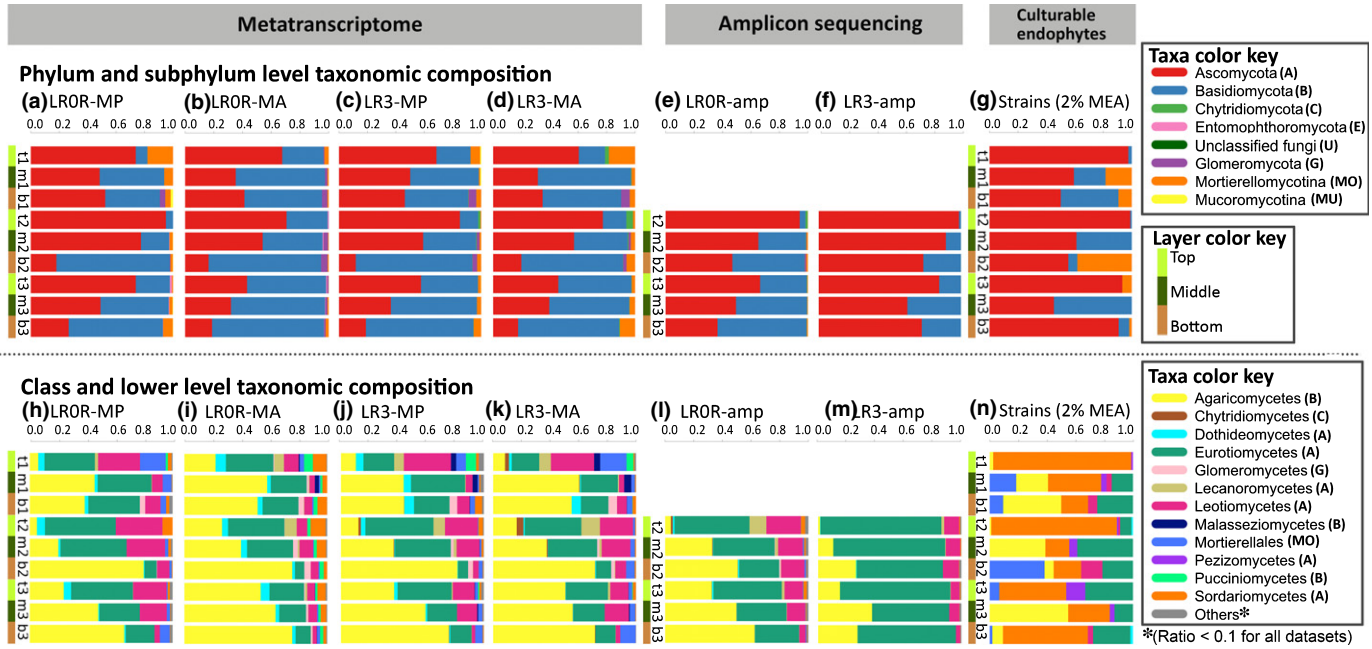

Fig. 4 Proportional distribution of fungal taxa based on metatranscriptomic rRNA data, amplicon sequencing and isolation of endophytes in culture at the (a–g) phylum–subphylum level and at the (h–n) class and lower taxonomic levels of *Dicranum scoparium*. If the taxonomic name could not be determined through MegaBlast + Megan, its lowest common ancestor (LCA) was used instead. Letters in parentheses in two of the legends represent abbreviations of the names of phyla or subphyla. MA, metatranscriptome assembled; MP, metatranscriptome pair-merged; amp, amplicon sequencing.

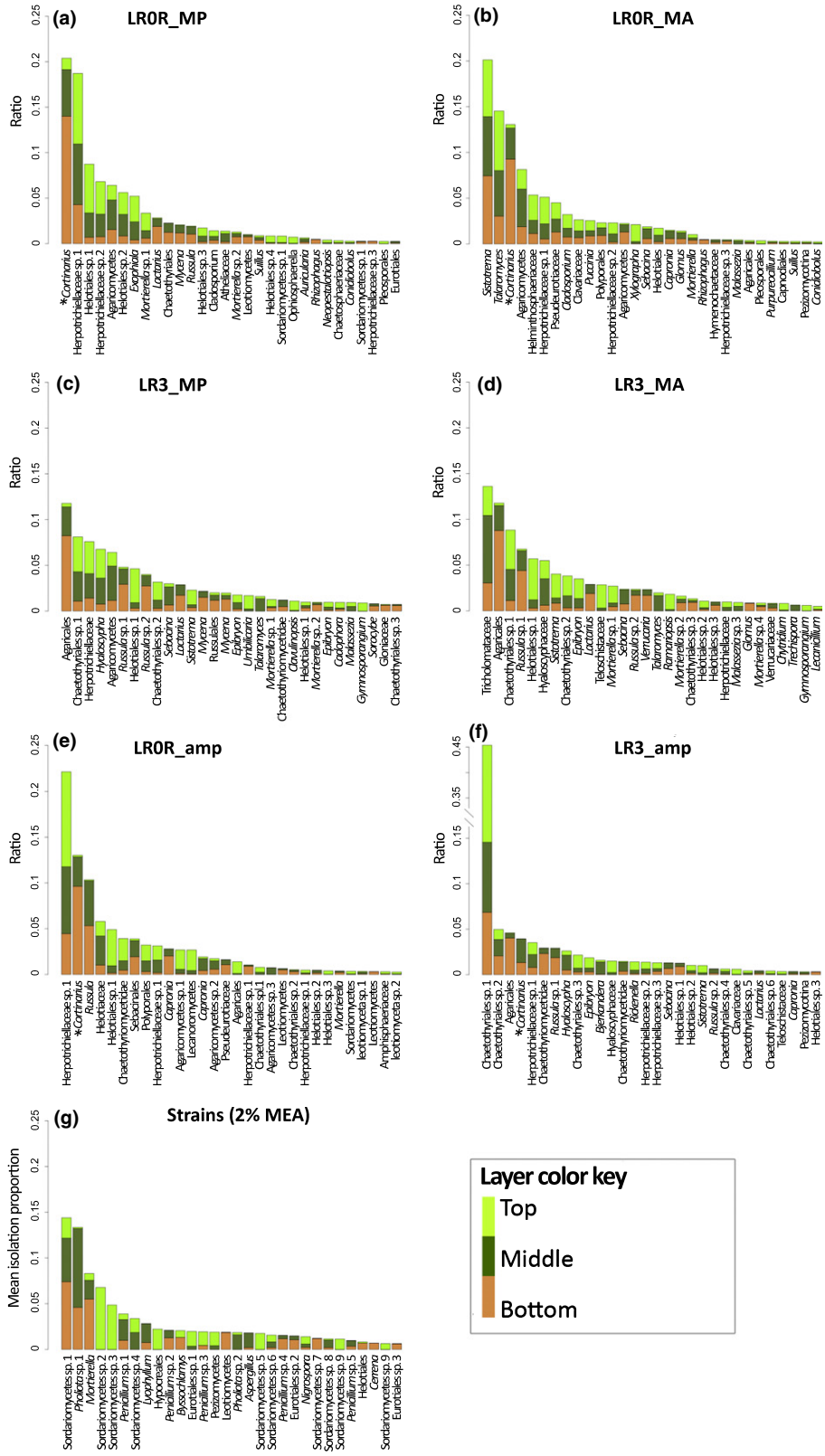

Fig. 5 Top 30 ranked abundances of fungi associated with *Dicranum scoparium*. The *y*-axes correspond to the mean ratios of reads mapped (a–f), and mean isolation proportions (g) of operational taxonomic units (OTUs) for the three microsites. Colors refer to specific layer fractions as shown in the legend. When the same taxon name appears more than once in one panel, this indicates the presence of multiple OTUs. **Cortinarius* = *Galerina*, see Supporting Information Methods S7. MA, metatranscriptome assembled; MP, metatranscriptome pair-merged; amp, amplicon sequencing).

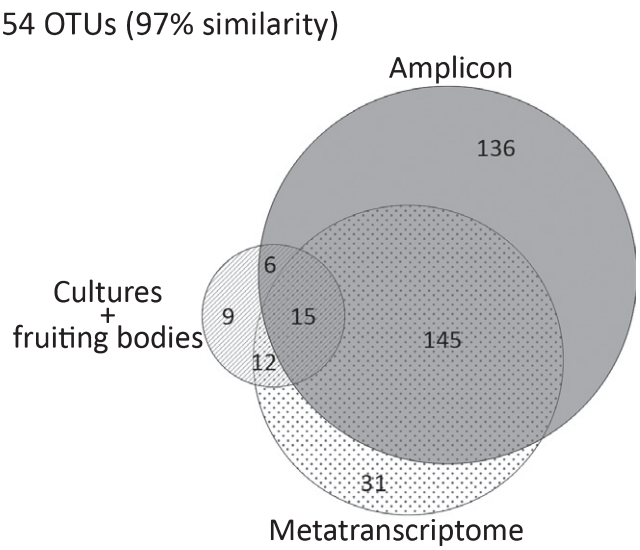

Fig. 6 Fungal operational taxonomic units (OTUs) detected by metatranscriptomics, amplicon sequencing, culturing and fruit-body collections of *Dicranum scoparium*. Venn diagram showing numbers of OTUs detected by each method using a 97% similarity threshold.

isolated in culture; Fig. 4h–n). Eurotiomycetes revealed by the metatranscriptome and amplicon sequencing were mostly Chaetothyriales, whereas those detected by culturing were mostly Eurotiales (Tables S7–S12).

Dominant fungal OTUs

Although the ranking order changed among datasets, OTUs representing Chaetothyriales (in some datasets classified to the family level as Herpotrichiellaceae) and Helotiales (in some datasets classified to the family level as Helotiaceae or to the genus *Hyaloscypha*) often were detected among the top five most abundant fungi based on metatranscriptomic and amplicon sequencing data (Fig. 5a–f). Cultures derived from surface-sterilized samples revealed three OTUs of Sordariomycetes among the top five most frequently isolated fungi (Fig. 5g).

OTU detection with metatranscriptomics, amplicon sequencing and culture isolations/fruit-body collections

Comparisons of the LR0R-MP, amplicon sequencing of LR0R, culturing and fruit-body data sets revealed 15 OTUs that were detected by all methods regardless of the sequence similarity threshold used (97%, Fig. 6; 95%, Fig. S8g). Amplicon sequencing detected the highest number of OTUs (302 OTUs at 97% similarity). Each method detected OTUs that were not detected by other methods (Fig. 6).

Discussion

RNAseq to assess living fungi in plants

Using a metatranscriptomic mapping approach, greater activity of fungi was detected in the middle and bottom layers of *D. scoparium* gametophytes relative to the top layer (Figs S2b, S3b). This is congruent with previous studies (Davey *et al.*, 2009, 2012, 2013a) in which a higher ergosterol content was detected in senescent vs living portions of mosses. Fungal communities in each portion of the senescence gradient were distinct, and the dissimilarities were mostly explained by species turnover, indicating that some fungi are strictly associated with certain trophic states (i.e. they are biotrophic vs saprotrophic). Fungi that colonize multiple layers were detected as well. Together, fungi with a single trophic state and those that might be multi-trophic make up the complex fungal communities associated with *D. scoparium*.

Ecological niche of taxa

The proportional ribosomal activities of Ascomycota are higher in the top layers vs middle and bottom layers of the moss holobiont (Fig. 4). By contrast, Basidiomycota are predominant and active in the lower layers compared to the top layer (Fig. 4). To tease apart whether one or both phyla caused this trend, we investigated read counts mapped to Ascomycota, Basidiomycota and non-Dikarya separately (Fig. S9). It is the increasing abundance of Basidiomycota toward the bottom layer, and their low abundance in the top layer, concurrent with a relatively stable Ascomycota abundance and activity across layers, that yields the Ascomycota–Basidiomycota trend (Figs 4, S9). These results suggest that *D. scoparium*-associated Ascomycota include endophytes/epiphytes that colonize the top photosynthetic layer, and saprotrophs that inhabit senescing or dead plant tissues. This reflects both a functional shift in the composition of ascomycete communities along the senescence gradient of this moss, and possibly the labile evolutionary histories of ascomycetous endophytes (i.e. closely related taxa can have different trophic modes) (Promputtha *et al.*, 2007; Arnold *et al.*, 2009). This can also be indicative of a multi-trophic characteristic for some ascomycetes (Osono & Hirose, 2011; Kuo *et al.*, 2014). By contrast, Basidiomycota were less frequently detected in photosynthetic tissues (see also Arnold, 2007) as endophytes but seemed to be an addition to the community in the bottom layers. We suggest that senescing moss tissues provide additional niches for these basidiomycetes. This overall trend demonstrates different functional guild utilizations by the two major fungal phyla associated with *D. scoparium*. Although communities differ on the whole among the layers, it is possible that some fungi detected as active in multiple layers might have a mycelium spanning all three layers of the moss. In this case, their activity in one part of the plant (e.g. top) may be fueled by absorptive nutrition and translocation from another part of the moss (e.g. middle or bottom). It is also possible that different portions of the same mycelium have different functions in different layers of the moss. The functions of different parts of the mycelium can be examined in future studies using *in vitro* co-culture experiments, for example.

Chaetothyriales and Helotiales represent two of the dominant lineages of Ascomycota in this study. Several species of Chaetothyriales and Helotiales have been proposed to have trophic modes ranging from biotrophy to saprotrophy (Davey & Currah, 2007; Kauserud *et al.*, 2008; Stenroos *et al.*, 2010), but

the nutritional modes of most remain undetermined. Our results demonstrate that several of these fungi are active across the three gametophytic layers, evidence that these fungi might be multi-trophic even within the same moss gametophyte. These results support the observation that many endophytes have saprotrophic lifestyles in addition to being symbiotrophic (Carroll & Petrini, 1983; Saikkonen *et al.*, 1998; Osono & Hirose, 2011; Zuccaro *et al.*, 2011; U'Ren & Arnold, 2016; Song *et al.*, 2017). Because no surface sterilization was conducted for the RNA-based approach, it is possible that some fungi detected using this method are epiphytes. Our finding that few active fungi were differentially more abundant in the top layer vs lower layers suggests that a small proportion of fungal endophytes are obligate biotrophs (Table S8), and that many are multi-trophic (see also U'Ren & Arnold, 2016). Whether this pattern results from directional turnover of communities (endophytes transitioning to saprotrophy from top to bottom, saprotrophs switching to endophytism from bottom to top, or individual mycelia spanning multiple layers but having different functional activity in each) requires further investigation.

The lichen-forming fungus *Xylographa*, a genus for which an evolutionary loss of the lichen symbiosis has been reported (Spribille *et al.*, 2014), was detected here as more active in the upper portion of *D. scoparium* (Fig. 3b). It has been hypothesized that mosses might serve as environmental reservoirs for lichen-forming fungi, allowing them to survive until appropriate algal partners are available (Davey & Currah, 2006). However, it seems more likely that colonization of mosses by this fungus is associated with the loss of the lichen symbiosis (Lutzoni *et al.*, 2001), which might have resulted from adaptation by the genus *Xylographa* to colonize exposed dead wood (Spribille *et al.*, 2014). Another possible explanation is that fungal spores in an early stage of germination or growth from nearby environments were sequenced unexpectedly.

Many of the basidiomycetous fungi detected in *D. scoparium* were ectomycorrhizal (ECM; e.g. *Russula*, *Lactarius*, *Suillus*). Typical mycorrhizal-like interactions between fungi and mosses are uncommon (Parke & Linderman, 1980; Zhang & Guo, 2007; Field *et al.*, 2015a). Given that our samples were collected in a forest that includes *Pinus taeda*, it is more plausible to us that these ECM fungi were pine-associated. The extending hyphal network from ECM–pine roots might benefit from nutrients released from decomposing portions of the gametophytes (Carleton & Read, 1991; Davey & Currah, 2006). Basidiomycetes such as *Rickenella* and *Sistotrema* were detected as active across all three moss layers, indicating their ability to engage in both saprotrophy and biotrophy (Kost, 1986).

Several OTUs belonging to Mortierellomycotina were detected in this study. Some appeared restricted to, or metabolically more active in, the nonphotosynthetic portion of *D. scoparium*, whereas others were active in all layers and thus appear to have a multi-trophic lifestyle (Figs 3, 4). Members of Mucoromycotina have been found in several surveys as endophytes in mosses (Osono *et al.*, 2012) and in soil (Tedersoo *et al.*, 2014), and some form mutualistic relationships with early embryophytes (e.g. liverworts) (Field *et al.*, 2015b). However, their functional interactions with mosses have not been examined closely.

Glomeromycetous fungi were only active in the bottom portion of *D. scoparium* (Figs 3, 4). Although arbuscular mycorrhizal fungi (AMF) are known to be associated with mosses, no mycorrhizal-like functions have been reported previously from mosses (Davey & Currah, 2006; Zhang & Guo, 2007; Liepiņa, 2012). It has been hypothesized that these AMF structures might be produced as extensions from nearby plants (Parke & Linderman, 1980). Given that *D. scoparium* has a thick tomentum and soil particles are probably attached to the gametophytes, it is possible that we are detecting AMF spores or hyphae in soils. Chytridiomycetous fungi were detected in this study, but at low abundances (Figs 3, 4). We suspect that these fungi may be living with algae associated with mosses (James *et al.*, 2006), or growing in soil particles. Similarly, the few fungi belonging to Entomophthoromycota are probably associated with arthropods on *D. scoparium* (Gryganskyi *et al.*, 2012). Other fungi with unknown ecology might also be detected accidentally, motivating further study.

RNA detection vs endophytes isolated in culture

RNA was obtained in this study without surface-sterilizing plant material, whereas the culture-based approach used surface-sterilized materials. This difference makes the direct comparison between RNA-derived data and culture-based data difficult. However, previous studies using culture-independent methods (454 pyrosequencing and cloning using nrITS DNA) based on water-cleaned moss samples (Kauserud *et al.*, 2008; Davey *et al.*, 2012, 2013a,b) revealed similar results to our RNA-based data: Chaetothyriales (Eurotiomycetes), Helotiales (Leotiomycetes) and Agaricales (Agaricomycetes) were dominant taxa. These parallels imply that the dominant fungal activities detected here are likely to be from fungi in close association with *D. scoparium*, rather than those living epiphytically or incidentally on the moss.

The fact that we cultured mostly Eurotiales whereas culture-independent methods detected members of the Chaetothyriales might indicate that the latter are obligate partners of mosses. These orders are in the subclasses Eurotiomycetidae and Chaetothyriomycetidae, respectively, of the class Eurotiomycetes (Lutzoni *et al.*, 2004; Geiser *et al.*, 2006; Gueidan *et al.*, 2008; Chen *et al.*, 2015). Contrary to Eurotiomycetidae, the subclass Chaetothyriomycetidae includes many lichen-forming fungi (most of which are obligate mutualists). This observation is consistent with the hypothesis that Chaetothyriales endophytes detected with culture-independent methods are functional associates of *D. scoparium*, and probably multi-trophic or strictly colonizing living mosses (Gueidan *et al.*, 2014) (Fig. 5). Another possible explanation is that these fungi do not grow on the MEA media used in this study.

The endophytes isolated after surface-sterilization were similar in composition to those obtained by culture-based sampling in other mosses, with Sordariomycetes being one of the most abundant classes (U'Ren *et al.*, 2010, 2012) and high isolation frequencies observed for Eurotiales and Mortierellomycotina (Osono *et al.*, 2012). Based on previous studies and our results, the great differences between RNA-based vs culture-based results

might lie in whether particular fungi are culturable, whether they can be dormant in the living plants, and the differences in the sampling depth (Fig. S10). The low activities (based on the abundance of rRNA transcripts) for some cultured fungi (e.g. Sordariomycetes) support the last of these. Nevertheless, there are still many fungi co-detected by RNA-based and culture-based methods on surface-sterilized materials (Fig. 6). In future work it would be ideal to have a surface-sterilization step in the transcriptomics pipeline, perhaps possible with the advancement of approaches for preparations that do not sacrifice RNA integrity.

Conclusion

By examining the living fungal components of the mycobiome along senescing gametophytes of the moss *D. scoparium*, we demonstrated that fungal communities in terms of the taxonomic composition of the biologically active fraction change across the senescence gradient. The shifts of fungal communities were mostly explained by species turnover, indicating that certain fungal OTUs may be strictly biotrophic (active only in the top photosynthetic layer) or saprotrophic (active only in the bottom decomposing layer). However, some fungal OTUs were detected as active across the senescence gradient, evidence of a multitrophic capability that may switch among individual mycelia, or within individual mycelia, in response to different states of plant tissue senescence. Regardless of the methodological approach used (metatranscriptome or RNA-based amplicon sequencing), similar overall trends were detected for beta diversity and community composition at higher taxonomic levels. Some OTU-level differences (e.g. taxonomic assignments) were observed. We conclude that metatranscriptomics is valid as a reliable approach for studying complex fungal communities, and can provide unique information about metabolically active proportions of fungal communities and plant mycobiomes.

Acknowledgements

We thank Jenny Li for help with obtaining cultures of endophytes and Steven Wu for assistance with bioinformatics. We thank Rytas Vilgalys, Danielle Armaleo and Jessica Nelson for valuable comments throughout the project. We thank Jana U'Ren and the Arnold lab (A.E.A.) for sharing the endophyte rRNA database. This project was funded by the National Science Foundation of America (NSF) grants DEB-1046065 and DEB-1541548 to F.L., DEB-1045766 to A.E.A., DBI-1046052 to Rytas Vilgalys, DEB-1737898 to G.B., and the NSF Doctoral Dissertation Improvement Grant (DEB-1701836) to K-H.C. and F.L. We also thank the Mycological Society of America for research awards and are grateful for support from Duke University to K-H.C.

Author contributions

K-H.C., H-L.L. and F.L. planned and designed the study. K-H.C. performed experiments and analyzed the data. G.B. developed the amplicon sequencing protocol. K-H.C., H-L.L., A.E.A., G.B. and F.L. wrote and revised the manuscript.

ORCID

Ko-Hsuan Chen http://orcid.org/0000-0001-9099-9054
Hui-Ling Liao http://orcid.org/0000-0002-1648-3444

References

Amend AS, Seifert KA, Bruns TD. 2010. Quantifying microbial communities with 454 pyrosequencing: does read abundance count? *Molecular Ecology* **19**: 5555–5565.

Anderson MJ. 2001. A new method for non-parametric multivariate analysis of variance. *Austral Ecology* **26**: 32–46.

Anderson IC, Genney DR, Alexander IJ. 2014. Fine-scale diversity and distribution of ectomycorrhizal fungal mycelium in a Scots pine forest. *New Phytologist* **201**: 1423–1430.

Arnold AE. 2007. Understanding the diversity of foliar endophytic fungi: progress, challenges, and frontiers. *Fungal Biology Reviews* **21**: 51–66.

Arnold AE, Miadlikowska J, Higgins KL, Sarvate SD, Gugger P, Way A, Hofstetter Vr, Kauff F, Lutzoni F. 2009. A phylogenetic estimation of trophic transition networks for ascomycetous fungi: are lichens cradles of symbiotrophic fungal diversification? *Systematic Biology* **58**: 283–297.

Baldrian P, Kolarik M, Stursova M, Kopecky J, Valaskova V, Vetrovsky T, Zifcakova L, Snajdr J, Ridl J, Vlcek C *et al.* 2012. Active and total microbial communities in forest soil are largely different and highly stratified during decomposition. *ISME Journal* **6**: 248–258.

Barnard RL, Osborne CA, Firestone MK. 2013. Responses of soil bacterial and fungal communities to extreme desiccation and rewetting. *ISME Journal* **7**: 2229–2241.

Baselga A. 2010. Partitioning the turnover and nestedness components of beta diversity. *Global Ecology and Biogeography* **19**: 134–143.

Bolger AM, Lohse M, Usadel B. 2014. Trimmomatic: a flexible trimmer for Illumina sequence data. *Bioinformatics* **30**: 2114–2120.

Bonito G, Reynolds H, Robeson MS, Nelson J, Hodkinson BP, Tuskan G, Schadt CW, Vilgalys R. 2014. Plant host and soil origin influence fungal and bacterial assemblages in the roots of woody plants. *Molecular Ecology* **23**: 3356–3370.

Brown DH, Bates JW. 1990. Bryophytes and nutrient cycling. *Botanical Journal of the Linnean Society* **104**: 129–147.

Caporaso JG, Kuczynski J, Stombaugh J, Bittinger K, Bushman FD, Costello EK, Fierer N, Pena AG, Goodrich JK, Gordon JI *et al.* 2010. QIIME allows analysis of high-throughput community sequencing data. *Nature Methods* **7**: 335–336.

Carleton TJ, Read DJ. 1991. Ectomycorrhizas and nutrient transfer in conifer-feather moss ecosystems. *Canadian Journal of Botany* **69**: 778–785.

Carroll G, Petrini O. 1983. Patterns of substrate utilization by some fungal endophytes from coniferous foliage. *Mycologia* **75**: 53–63.

Chen K-H, Miadlikowska J, Molnár K, Arnold AE, U'Ren JM, Gaya E, Gueidan C, Lutzoni F. 2015. Phylogenetic analyses of eurotiomycetous endophytes reveal their close affinities to Chaetothyriales, Eurotiales, and a new order -Phaeomoniellales. *Molecular Phylogenetics and Evolution* **85**: 117–130.

Choma M, Bárta J, Šantrůčková H, Urich T. 2016. Low abundance of Archaeorhizomycetes among fungi in soil metatranscriptomes. *Scientific Reports* **6**: 38455.

Davey ML, Currah RS. 2006. Interactions between mosses (Bryophyta) and fungi. *Canadian Journal of Botany* **84**: 1509–1519.

Davey ML, Currah RS. 2007. A new species of *Cladophialophora* (hyphomycetes) from boreal and montane bryophytes. *Mycological Research* **111**: 106–116.

Davey ML, Heegaard E, Halvorsen R, Kauserud H, Ohlson M. 2013a. Amplicon-pyrosequencing-based detection of compositional shifts in bryophyte-associated fungal communities along an elevation gradient. *Molecular Ecology* **22**: 368–383.

Davey ML, Heegaard E, Halvorsen R, Ohlson M, Kauserud H. 2012. Seasonal trends in the biomass and structure of bryophyte-associated fungal communities explored by 454 pyrosequencing. *New Phytologist* **195**: 844–856.

Davey ML, Heimdal R, Ohlson M, Kauserud H. 2013b. Host- and tissue-specificity of moss-associated *Galerina* and *Mycena* determined from amplicon pyrosequencing data. *Fungal Ecology* **6**: 179–186.

Davey ML, Nybakken L, Kauserud H, Ohlson M. 2009. Fungal biomass associated with the phyllosphere of bryophytes and vascular plants. *Mycological Research* **113**: 1254–1260.

Davey ML, Skogen MJ, Heegaard E, Halvorsen R, Kauserud H, Ohlson M. 2017. Host and tissue variations overshadow the response of boreal moss-associated fungal communities to increased nitrogen load. *Molecular Ecology* **26**: 571–588.

Davey ML, Tsuneda A, Currah RS. 2010. Saprobic and parasitic interactions of *Coniochaeta velutina* with mosses. *Botany-Botanique* **88**: 258–265.

Davison J, Moora M, Öpik M, Adholeya A, Ainsaar L, Bâ A, Burla S, Diedhiou AG, Hiiesalu I, Jairus T *et al.* 2015. Global assessment of arbuscular mycorrhizal fungus diversity reveals very low endemism. *Science* **349**: 970–973.

Edgar RC. 2013. UPARSE: highly accurate OTU sequences from microbial amplicon reads. *Nature Methods* **10**: 996–998.

Field KJ, Pressel S, Duckett JG, Rimington WR, Bidartondo MI. 2015a. Symbiotic options for the conquest of land. *Trends in Ecology and Evolution* **30**: 477–486.

Field KJ, Rimington WR, Bidartondo MI, Allinson KE, Beerling DJ, Cameron DD, Duckett JG, Leake JR, Pressel S. 2015b. First evidence of mutualism between ancient plant lineages (Haplomitriopsida liverworts) and Mucoromycotina fungi and its response to simulated Palaeozoic changes in atmospheric CO_2. *New Phytologist* **205**: 743–756.

Gardes M, Bruns TD. 1993. ITS primers with enhanced specificity for basidiomycetes – application to the identification of mycorrhizae and rusts. *Molecular Ecology* **2**: 113–118.

Geisen S, Tveit AT, Clark IM, Richter A, Svenning MM, Bonkowski M, Urich T. 2015. Metatranscriptomic census of active protists in soils. *ISME Journal* **9**: 2178–2190.

Geiser DM, Gueidan C, Miadlikowska J, Lutzoni F, Kauff F, Hofstetter V, Fraker E, Schoch CL, Tibell L, Untereiner WA *et al.* 2006. Eurotiomycetes: Eurotiomycetidae and Chaetothyriomycetidae. *Mycologia* **98**: 1053–1064.

Gryganskyi AP, Humber RA, Smith ME, Miadlikovska J, Wu S, Voigt K, Walther G, Anishchenko IM, Vilgalys R. 2012. Molecular phylogeny of the Entomophthoromycota. *Molecular Phylogenetics and Evolution* **65**: 682–694.

Gueidan C, Aptroot A, da Silva Cáceres M, Badali H, Stenroos S. 2014. A reappraisal of orders and families within the subclass Chaetothyriomycetidae (Eurotiomycetes, Ascomycota). *Mycological Progress* **13**: 1027–1039.

Gueidan C, Ruibal C, de Hoog GS, Gorbushina AA, Untereiner WA, Lutzoni F. 2008. A rock-inhabiting ancestor for mutualistic and pathogen-rich fungal lineages. *Studies in Mycology* **61**: 111–119.

Hesse CN, Mueller RC, Vuyisich M, Gallegos-Graves LV, Gleasner CD, Zak DR, Kuske CR. 2015. Forest floor community metatranscriptomes identify fungal and bacterial responses to N deposition in two maple forests. *Frontiers in Microbiology* **6**: 337.

Huson DH, Auch AF, Qi J, Schuster SC. 2007. MEGAN analysis of metagenomic data. *Genome Research* **17**: 377–386.

James TY, Letcher PM, Longcore JE, Mozley-Standridge SE, Porter D, Powell MJ, Griffith GW, Vilgalys R. 2006. A molecular phylogeny of the flagellated fungi (Chytridiomycota) and description of a new phylum (Blastocladiomycota). *Mycologia* **98**: 860–871.

Katoh K, Standley DM. 2013. MAFFT multiple sequence alignment software version 7: improvements in performance and usability. *Molecular Biology and Evolution* **30**: 772–780.

Kauserud H, Mathiesen C, Ohlson M. 2008. High diversity of fungi associated with living parts of boreal forest bryophytes. *Botany-Botanique* **86**: 1326–1333.

Kost G. 1986. Morphology, anatomy and biology of species of the genus *Rickenella*. Atti del Convegno Internazionale del 10-15 settembre 1984. Borgo Val di Taro – Italy. *Atti del Centro Studi per la Flora Mediterranea* **6**: 63–81.

Kuo H-C, Hui S, Choi J, Asiegbu FO, Valkonen JPT, Lee Y-H. 2014. Secret lifestyles of *Neurospora crassa*. *Scientific Reports* **4**: 5135.

Langmead B, Trapnell C, Pop M, Salzberg SL. 2009. Ultrafast and memory-efficient alignment of short DNA sequences to the human genome. *Genome Biology* **10**: R25.

Lenton TM, Dahl TW, Daines SJ, Mills BJW, Ozaki K, Saltzman MR, Porada P. 2016. Earliest land plants created modern levels of atmospheric oxygen. *Proceedings of the National Academy of Sciences, USA* **113**: 9704–9709.

Lesniewski RA, Jain S, Anantharaman K, Schloss PD, Dick GJ. 2012. The metatranscriptome of a deep-sea hydrothermal plume is dominated by water column methanotrophs and lithotrophs. *ISME Journal* **6**: 2257–2268.

Li F-W, Villarreal JC, Kelly S, Rothfels CJ, Melkonian M, Frangedakis E, Ruhsam M, Sigel EM, Der JP, Pittermann J *et al.* 2014. Horizontal transfer of an adaptive chimeric photoreceptor from bryophytes to ferns. *Proceedings of the National Academy of Sciences, USA* **111**: 6672–6677.

Liao H-L, Chen Y, Bruns TD, Peay KG, Taylor JW, Branco S, Talbot JM, Vilgalys R. 2014. Metatranscriptomic analysis of ectomycorrhizal roots reveal genes associated with *Piloderma–Pinus* symbiosis: improved methodologies for assessing gene expression *in situ*. *Environmental Microbiology* **16**: 3730–3742.

Liepiņa L. 2012. Occurrence of fungal structures in bryophytes of the boreo-nemoral zone. *Environmental and Experimental Biology* **10**: 35–40.

Lindahl BD, Nilsson RH, Tedersoo L, Abarenkov K, Carlsen T, Kjøller R, Kõljalg U, Pennanen T, Rosendahl S, Stenlid J *et al.* 2013. Fungal community analysis by high-throughput sequencing of amplified markers – a user's guide. *New Phytologist* **199**: 288–299.

Lindo Z, Gonzalez A. 2010. The Bryosphere: an integral and influential component of the earth's biosphere. *Ecosystems* **13**: 612–627.

Liu K-L, Porras-Alfaro A, Kuske CR, Eichorst SA, Xie G. 2012. Accurate, rapid taxonomic classification of fungal large-subunit rRNA genes. *Applied and Environmental Microbiology* **78**: 1523–1533.

Love M, Huber W, Anders S. 2014. Moderated estimation of fold change and dispersion for RNA-seq data with DESeq2. *Genome Biology* **15**: 550.

Lundberg DS, Yourstone S, Mieczkowski P, Jones CD, Dangl JL. 2013. Practical innovations for high-throughput amplicon sequencing. *Nature Methods* **10**: 999–1002.

Lutzoni F, Kauff F, Cox CJ, McLaughlin D, Celio G, Dentinger B, Padamsee M, Hibbett D, James TY, Baloch E. 2004. Assembling the fungal tree of life: progress, classification, and evolution of subcellular traits. *American Journal of Botany* **91**: 1460–1480.

Lutzoni F, Pagel M, Reeb V. 2001. Major fungal lineages are derived from lichen symbiotic ancestors. *Nature* **411**: 937–940.

Martínez-Abaigar J, Núñez-Olivera E, Matcham HW, Duckett JG. 2005. Interactions between parasitic fungi and mosses: pegged and swollen-tipped rhizoids in *Funaria* and *Bryum*. *Journal of Bryology* **27**: 47–53.

Marx DH. 1969. The influence of ectotrophic mycorrhizal fungi on the resistance of pine roots to pathogenic infections. I. Antagonism of mycorrhizal fungi to root pathogenic fungi and soil bacteria. *Phytopathology* **59**: 153–163.

Mueller RC, Gallegos-Graves LV, Kuske CR. 2016. A new fungal large subunit ribosomal RNA primer for high-throughput sequencing surveys. *FEMS Microbiology Ecology* **92**: pii: fiv153.

Mueller RC, Gallegos-Graves L, Zak DR, Kuske CR. 2015. Assembly of active bacterial and fungal communities along a natural environmental gradient. *Microbial Ecology* **71**: 57–67.

Nguyen NH, Smith D, Peay K, Kennedy P. 2015. Parsing ecological signal from noise in next generation amplicon sequencing. *New Phytologist* **205**: 1389–1393.

Oksanen J, Blanchet FG, Kindt R, Legendre P, Minchin PR, O'Hara RB, Simpson GL, Solymos P, Stevens MHH, Wagner H. 2015. *vegan: Community ecology package*. R package version 2.3-2. URL http://cran.r-project.org/package=vegan.

Oono R, Lutzoni F, Arnold AE, Kaye L, U'Ren JM, May G, Carbone I. 2014. Genetic variation in horizontally transmitted fungal endophytes of pine needles reveals population structure in cryptic species. *American Journal of Botany* **101**: 1362–1374.

Osono T, Hirose D. 2011. Colonization and lignin decomposition of pine needle litter by *Lophodermium pinastri*. *Forest Pathology* **41**: 156–162.

Osono T, Ueno T, Uchida M, Kanda H. 2012. Abundance and diversity of fungi in relation to chemical changes in arctic moss profiles. *Polar Science* **6**: 121–131.

Parke JL, Linderman RG. 1980. Association of vesicular-arbuscular mycorrhizal fungi with the moss *Funaria hygrometrica*. *Canadian Journal of Botany* **58**: 1898–1904.

Peay KG, Kennedy PG, Talbot JM. 2016. Dimensions of biodiversity in the Earth mycobiome. *Nature Reviews Microbiology* **14**: 434–447.

Porras-Alfaro A, Liu K-L, Kuske CR, Xie G. 2014. From genus to phylum: large-subunit and internal transcribed spacer rRNA operon regions show similar classification accuracies influenced by database composition. *Applied and Environmental Microbiology* **80**: 829–840.

Promputtha I, Lumyong S, Dhanasekaran V, McKenzie E, Hyde K, Jeewon R. 2007. A phylogenetic evaluation of whether endophytes become saprotrophs at host senescence. *Microbial Ecology* **53**: 579–590.

Rajala T, Peltoniemi M, Hantula J, Raisa M, Pennanen T. 2011. RNA reveals a succession of active fungi during the decay of Norway spruce logs. *Fungal Ecology* **4**: 437–448.

Redhead SA. 1981. Parasitism of bryophytes by agarics. *Canadian Journal of Botany* **59**: 63–67.

Robinson MD, McCarthy DJ, Smyth GK. 2009. edgeR: a Bioconductor package for differential expression analysis of digital gene expression data. *Bioinformatics* **26**: 139–140.

Saikkonen K, Faeth SH, Helander M, Sullivan TJ. 1998. Fungal endophytes: a continuum of interactions with host plants. *Annual Review of Ecology, Evolution, and Systematics* **29**: 319–343.

Schoch CL, Seifert KA, Huhndorf S, Robert V, Spouge JL, Levesque CA, Chen W, Fungal Barcoding C. 2012. Nuclear ribosomal internal transcribed spacer (ITS) region as a universal DNA barcode marker for Fungi. *Proceedings of the National Academy of Sciences, USA* **109**: 6241–6246.

Seifert KA. 2009. Progress towards DNA barcoding of fungi. *Molecular Ecology Resources* **9**: 83–89.

Song Z, Kennedy PG, Liew FJ, Schilling JS. 2017. Fungal endophytes as priority colonizers initiating wood decomposition. *Functional Ecology* **31**: 407–418.

Spribille T, Resl P, Ahti T, Pérez-Ortega S, Tønsberg T, Mayrhofer H, Lumbsch HT. 2014. Molecular systematics of the wood-inhabiting, lichen-forming genus *Xylographa* (Baeomycetales, Ostropomycetidae) with eight new species. *Acta Universitatis Upsaliensis. Symbolae botanicae Upsalienses: Arbeten fran Botaniska institutionerna i Uppsala* **37**: 1–87.

Stenroos S, Laukka T, Huhtinen S, Döbbeler P, Myllys L, Syrjänen K, Hyvönen J. 2010. Multiple origins of symbioses between ascomycetes and bryophytes suggested by a five-gene phylogeny. *Cladistics* **26**: 281–300.

Tedersoo L, Anslan S, Bahram M, PÃµlme S, Riit T, Liiv I, KÃµljalg U, Kisand V, Nilsson H, Hildebrand F *et al.* 2015. Shotgun metagenomes and multiple primer pair-barcode combinations of amplicons reveal biases in metabarcoding analyses of fungi. *MycoKeys* **10**: 1–43.

Tedersoo L, Bahram M, Põlme S, Kõljalg U, Yorou NS, Wijesundera R, Ruiz LV, Vasco-Palacios AdM, Thu PQ, Suija A *et al.* 2014. Global diversity and geography of soil fungi. *Science* **346**: 6213.

Turetsky MR, Bond-Lamberty B, Euskirchen E, Talbot J, Frolking S, McGuire AD, Tuittila ES. 2012. The resilience and functional role of moss in boreal and arctic ecosystems. *New Phytologist* **196**: 49–67.

U'Ren JM, Arnold AE. 2016. Diversity, taxonomic composition, and functional aspects of fungal communities in living, senesced, and fallen leaves at five sites across North America. *PeerJ* **4**: e2768.

U'Ren JM, Dalling JW, Gallery RE, Maddison DR, Davis EC, Gibson CM, Arnold AE. 2009. Diversity and evolutionary origins of fungi associated with seeds of a neotropical pioneer tree: a case study for analysing fungal environmental samples. *Mycological Research* **113**: 432–449.

U'Ren JM, Lutzoni F, Miadlikowska J, Arnold AE. 2010. Community analysis reveals close affinities between endophytic and endolichenic fungi in mosses and lichens. *Microbial Ecology* **60**: 340–353.

U'Ren JM, Lutzoni F, Miadlikowska J, Laetsch AD, Arnold AE. 2012. Host and geographic structure of endophytic and endolichenic fungi at a continental scale. *American Journal of Botany* **99**: 898–914.

U'Ren JM, Riddle JM, Monacell JT, Carbone I, Miadlikowska J, Arnold AE. 2014. Tissue storage and primer selection influence pyrosequencing-based inferences of diversity and community composition of endolichenic and endophytic fungi. *Molecular Ecology Resources* **14**: 1032–1048.

Vilgalys R, Hester M. 1990. Rapid genetic identification and mapping of enzymatically amplified ribosomal DNA from several *Cryptococcus* species. *Journal of Bacteriology* **172**: 4238–4246.

Yu N, Kim JA, Jeong M-H, Cheong Y, Hong S, Jung J, Koh Y, Hur J-S. 2014. Diversity of endophytic fungi associated with bryophyte in the maritime Antarctic (King George Island). *Polar Biology* **37**: 27–36.

Yuan Z, Chen L. 2014. The role of endophytic fungal individuals and communities in the decomposition of *pinus massoniana* needle litter. *PLoS ONE* **9**: e105911.

Zerbino DR, Birney E. 2008. Velvet: algorithms for *de novo* short read assembly using de Bruijn graphs. *Genome Research* **18**: 821–829.

Zhang Y, Guo L-D. 2007. Arbuscular mycorrhizal structure and fungi associated with mosses. *Mycorrhiza* **17**: 319–325.

Zimmer AD, Lang D, Buchta K, Rombauts S, Nishiyama T, Hasebe M, Van de Peer Y, Rensing SA, Reski R. 2013. Reannotation and extended community resources for the genome of the non-seed plant *Physcomitrella patens* provide insights into the evolution of plant gene structures and functions. *BMC Genomics* **14**: 1–20.

Zuccaro A, Lahrmann U, Güldener U, Langen G, Pfiffi S, Biedenkopf D, Wong P, Samans B, Grimm C, Basiewicz M *et al.* 2011. Endophytic life strategies decoded by genome and transcriptome analyses of the mutualistic root symbiont *Piriformospora indica*. *PLoS Pathogens* **7**: e1002290.

Supporting Information

Additional Supporting Information may be found online in the Supporting Information tab for this article:

Fig. S1 Quality filtering of cDNA amplicon sequencing.

Fig. S2 Workflow for metatranscriptome LR0R database.

Fig. S3 Workflow for metatranscriptome LR3 database.

Fig. S4 Ratio of the metatranscriptomic data mapping to the reference plant genome/transcriptome.

Fig. S5 Isolation frequency of fungal and bacterial endophytes in culture.

Fig. S6 Fungal hyphae in photosynthetic tissues of *Dicranum scoparium*.

Fig. S7 Fruit-bodies collected at the sampling site.

Fig. S8 Results from the LR3-MA dataset when using an OTU delimitation of 95% similarity.

Fig. S9 Ratio of reads mapped to Ascomycota, Basidiomycota and non-Dikarya phyla based on the LR0R-MP dataset.

Fig. S10 Rarefaction curves of all datasets.

Table S1 Primer sequences for 1st (original LR0R, LR3) and 2nd (frame-shift tagging) PCR steps in preparation of MiSeq amplicon sequencing libraries

Table S2 Sequences of index-tagging primers used in the 3rd PCR steps for MiSeq amplicon sequencing libraries

Table S3 Sequencing primers submitted for Illumina MiSeq amplicon sequencing

Table S4 Summary of RNA extraction quality and RNAseq results across layers

Table S5 Results of chi-square test for mapped read ratios of fungi across layers

Table S6 ADONIS results for testing layer effect on beta diversity

Table S7 LR0R-MP OTU table and detailed results of the Wald test

Table S8 LR0R-MA OTU table and detailed results of the Wald test

Table S9 LR3-MP OTU table and detailed results of the Wald test

Table S10 LR3-MA OTU table and detailed results of the Wald test

Table S11 Amplicon sequencing LR0R OTU table

Table S12 Amplicon sequencing LR3 OTU table

Table S13 Turnover and nested components of beta diversity based on Sørensen index

Table S14 Summary of Wald test results of four different datasets (LR0R-MA, LR0R-MP, LR3-MA, LR3-MP)

Table S15 OTU table of endophytes isolated in culture and putative taxonomy based on MegaBlast against GenBank

Table S16 Strain information for endophytes isolated in culture

Table S17 Fruit-body collections from *Dicranum scoparium* at the collection site for this study

Table S18 Results of two-way ANOVA test across layers at phylum and subphylum levels

Table S19 Results of one-way ANOVA test of reads mapped to individual phylum/subphylum levels across layers

Methods S1 RNAseq library preparation.

Methods S2 nrLSU cDNA library preparation for amplicon sequencing.

Methods S3 Additional information on RNAseq data quality checking and processing.

Methods S4 MiSeq amplicon sequence processing.

Methods S5 Scripts for bioinformatics.

Methods S6 Primary and secondary reference database constructions.

Methods S7 Comparison between metatranscriptome vs amplicon sequencing regarding fungal community assessment with plant.

Please note: Wiley Blackwell are not responsible for the content or functionality of any Supporting Information supplied by the authors. Any queries (other than missing material) should be directed to the *New Phytologist* Central Office.